THE JOURNAL OF PHYSICAL CHEMISTRY A

Article

pubs.acs.org/JPCA

Thermochemistry of the Reaction of SF_6 with Gas-Phase Hydrated Electrons: A Benchmark for Nanocalorimetry

Amou Akhgarnusch,[†,‡] Robert F. Höckendorf,[†] and Martin K. Beyer*[,†,‡]

[†]Institut für Physikalische Chemie, Christian-Albrechts-Universität zu Kiel, Olshausenstrasse 40, 24098 Kiel, Germany

[‡]Institut für Ionenphysik und Angewandte Physik, Leopold-Franzens-Universität Innsbruck, Technikerstrasse 25, 6020 Innsbruck, Austria

Supporting Information

ABSTRACT: The reaction of sulfur hexafluoride with gas-phase hydrated electrons $(H_2O)_n^-$, $n \approx 60-130$, is investigated at temperatures T = 140−300 K by Fourier transform ion cyclotron resonance (FT-ICR) mass spectrometry. SF_6 reacts with a temperature-independent rate of $3.0 \pm 1.0 \times 10^{-10}$ cm^3 s^{-1} via exclusive formation of the hydrated F^- anion and the $SF_5^\bullet$ radical, which evaporates from the cluster. Nanocalorimetry yields a reaction enthalpy of $\Delta H_{R,298K} = 234 \pm 24$ kJ mol^{-1}. Combined with literature thermochemical data from bulk aqueous solution, these result in an F_5S-F bond dissociation enthalpy of $\Delta H_{298K} = 455 \pm 24$ kJ mol^{-1}, in excellent agreement with all high-level quantum chemical calculations in the literature. A combination with gas-phase literature thermochemistry also yields an experimental value for the electron affinity of $SF_5^\bullet$, $EA(SF_5^\bullet) = 4.27 \pm 0.25$ eV.

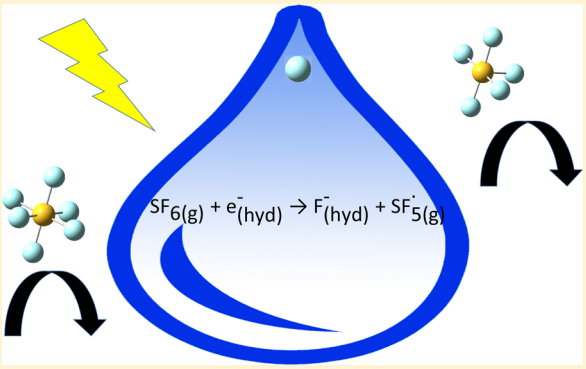

1. INTRODUCTION

Because of its high electron affinity, low toxicity, and chemical stability, SF_6 finds a wide range of technological applications, for example, as an electron scavenger in electrical switching devices and plasma reactors and in the electrical power industry as an insulator for gas-insulated equipment in power stations.[1−4] On the contrary, sulfur hexafluoride is also considered to be a very potent greenhouse gas. It has a very long residence lifetime, and it is inert to chemical or photolytic degradation.[5−8] The concentration of the efficient infrared absorber in the atmosphere has increased in recent years.[9] Not surprisingly, SF_6 has been studied extensively in the gas phase.[10−15] Particularly well investigated are electron attachment reactions of SF_6 in the gas phase.[3,16−23] Low-energy electrons generate the stable anion SF_6^-, while the formation of SF_5^- is endothermic by 0.4 eV.[22] The determination of the exact adiabatic electron affinity (EA_{ad}) has proven difficult.[23−28] A third-law analysis by Troe, Miller, and Viggiano,[23] using high-precision calculations of SF_6^- harmonic frequencies and anharmonicities by Eisfeld,[29,30] provided the most reliable value to date, $EA(SF_6) = 1.03 \pm 0.05$ eV. This is in remarkable agreement with the calculations by Karton and Martin near the relativistic CCSDT(Q) basis set limit, who report $EA(SF_6) = 1.0340 \pm 0.03$ eV.[31]

The ground state of the neutral as well as the anion was long thought to have octahedral geometry with O_h symmetry.[32] Recent calculations by Eisfeld corroborate this view for the neutral, with an S−F bond length of 1.56 Å, while the anion actually has C_{4v} symmetry, with the two axial S−F bonds elongated asymmetrically to 1.68 and 1.93 Å, while the equatorial S−F bond lengths remain at 1.60 Å.[29] High-level ab initio calculations consistently predict the F_5S-F bond energy at 0 K as 438−447 kJ mol^{-1},[33−38] significantly higher than all experimental values,[39,40] as previously discussed.[33,34] The most realistic experimental value seems to be the re-evaluation by Tsang and Herron,[40] giving a 298 K value of 420 ± 10 kJ mol^{-1}.

The anion in the gas phase undergoes decomposition reactions, depending on the kinetic energy of the electron and the thermal energy of the neutral SF_6,[41−44] exhibiting distinct resonances.[21] With thermal SF_6 and electron kinetic energies below 2 eV, the formation of the SF_5^- anion and the $F^\bullet$ radical is preferred,[22,44,45] with a threshold of 0.2 eV.[44] At higher energies, the production of F^- and $SF_5^\bullet$ species becomes dominant.[46,47] At even higher energies, more and more decomposition channels open up, leading to SF_4^-, SF_3^-, SF_2, F_2^-, and so on.[48−50] Ion−molecule reactions with SF_6^- frequently proceed via fluoride transfer,[51] while collision-induced dissociation predominantly results in the formation of $SF_5^- + F^\bullet$.[52] Interestingly, ion−molecule reactions of SF_6^- with H_2O at pressures of 50−500 Torr result in the formation of SOF_4^- and $F^-(HF)_2$.[53] In the reaction of SF_6 with the hydrated electron in bulk aqueous solution, the primary reaction step is fluoride formation.[54,55] Subsequent hydrolysis

Received: July 19, 2015
Revised: September 10, 2015
Published: September 10, 2015

DOI: 10.1021/acs.jpca.5b06975
J. Phys. Chem. A 2015, 119, 9978−9985

of $SF_5^•$ leads to the formation of five more fluoride ions as well as HSO_3^-, $6H_3O^+$, and $OH^•$.[54]

Using thermochemical data from cluster studies to extrapolate to bulk thermochemistry has a long tradition, including hydration enthalpies of the fluoride ion.[56−58] In the present study, we go in the opposite direction, using thermochemical data from bulk aqueous solution to infer gas-phase thermochemistry. We examine the reaction of SF_6 with gas-phase hydrated electrons $(H_2O)_n^-$ at different temperatures over a size range of $n \approx 60-130$. We have previously shown that nanocalorimetry[59−67] in combination with literature thermochemistry for bulk aqueous phase yields quantitatively consistent results for gas-phase reaction enthalpies.[65] Here we extend this idea to derive the F_5S-F bond dissociation energy as well as the adiabatic electron affinity of $SF_5^•$ from the results of nanocalorimetry.

2. EXPERIMENTAL SETUP

The experiments are conducted on a modified Bruker/Spectroscopin CMS47X FT-ICR mass spectrometer equipped with a 4.7 T superconducting magnet, a modified Bruker infinity cell, which enables-temperature resolved measurements,[68] and an APEX III data station.[64,69−71] An external laser vaporization source[72−74] generates hydrated electrons by laser vaporization of a solid zinc target and supersonic expansion of the hot plasma in a 50 μs long helium/water gas pulse.[75,76] The hydrated electrons are transferred via an electrostatic lens system through differential pumping stages into the ultrahigh vacuum (UHV) region of the mass spectrometer, where they are stored in the ICR cell at a base pressure below 5×10^{-10} mbar. The SF_6 gas (Sigma-Aldrich, 99.75% purity) is introduced into the UHV region through a needle valve at a constant pressure of typically 9.9×10^{-9} mbar. The cell is cooled with liquid nitrogen, and the temperature is adjusted via the flow rate. Reactions are monitored by recording mass spectra as a function of time.

The intensities of reactant and product clusters in the mass spectra are corrected for the natural abundance of ^2H and ^{18}O and summed over all cluster sizes to analyze the kinetics and the thermochemistry of the reaction. The kinetic fit yielded a pseudo-first-order rate k_{rel} [s^{-1}], which is converted to the absolute reaction rate k_{abs} as previously described.[77] The effect of the base pressure on the pressure reading is neglected because it is <5% of the total pressure. For the derived absolute rate constants, a relative error of ±25% is assumed, determined by the uncertainty of the pressure calibration.

To extract the reaction enthalpy from these data, the average cluster sizes N_R and N_P of reactant and product species, respectively, are calculated. The results are fitted with a genetic algorithm with the following differential equations

$$dN_R = -k_f(N_R - N_{0,R})\,dt \quad (1)$$

$$dN_P = -k_f(N_P - N_{0,P})\,dt + (N_R - \Delta N_{vap} - N_P)\left(\frac{kI_R}{I_P}\right)dt \quad (2)$$

Equation 1 and the first term in eq 2 describe the blackbody radiation induced dissociation (BIRD) of water clusters,[78−84] with k_f describing the linear dependence on cluster size. $N_{0,R}$ and $N_{0,P}$ account for the contribution of the ionic core to the infrared absorption cross sections. The second term in eq 2 describes the evaporation of water molecules due to the reaction enthalpy released in the water cluster. The average number of evaporated water molecules ΔN_{vap} is the key result of the fit. The energy required to evaporate a water molecule from the cluster, $\Delta E_{vap} = 43.3 \pm 3.1$ kJ mol^{-1}, has been measured by photo dissociation.[85,86] Our original fit procedure required us to keep one fit parameter fixed to reach convergence.[64] We now fit the average cluster size as well as the difference in cluster size over the full time range. With this modification of the fit procedure, robust convergence of the fits is achieved with all fit parameters active.

3. RESULTS AND DISCUSSION

Mass spectra of the reaction of SF_6 with $(H_2O)_n^-$ at 298 K are displayed in Figure 1. Because of the fill cycle of the ICR cell, which takes 2 s, reaction products are present at nominally 0 s reaction delay, that is, immediately after completing the fill cycle.

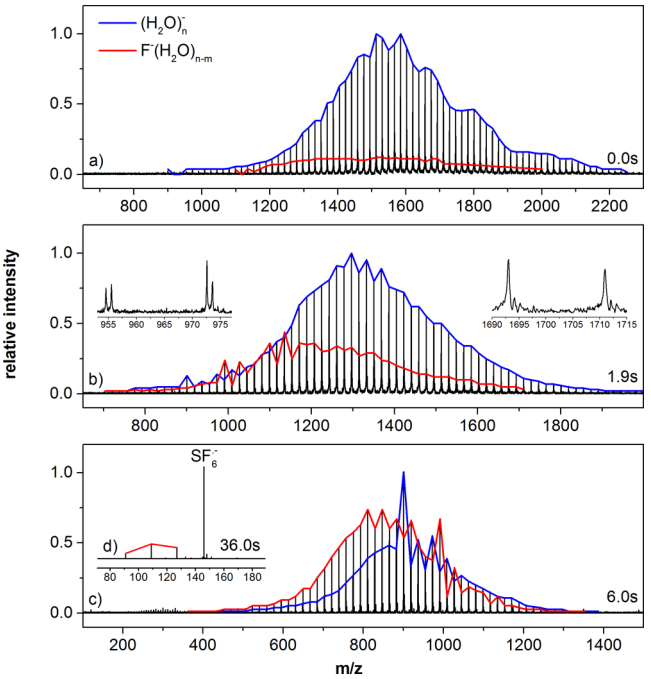

Figure 1. Mass spectra of the reaction of SF_6 with hydrated electrons (blue) after (a) 0.0, (b) 1.9, (c) 6.0, and (d) 36.0 s. The most intense peak, the $SF_6^{•-}$ anion, is ejected by resonant excitation from the ICR cell, except for the experiment shown in panel d. Products (red) are present already at nominal 0.0 s due to the 2 s filling cycle. Both species undergo BIRD and continuously lose water ligands. After 6.0 s the product cluster starts to dominate. Magic cluster sizes are observed in the size regime $n \approx 50-60$, in particular, $(H_2O)_{50}^-$ and $F^-(H_2O)_{54}$. After 36.0 s the reaction is completed. Besides $SF_6^{•-}$, $F^-(H_2O)_k$ with $k = 4-6$ is observed.

Hydrated electrons react quantitatively by the formation of $F^-(H_2O)_{n-m}$, eq 3. Clearly visible is the loss of water molecules due to BIRD, which rapidly shifts the cluster size distribution to smaller values. It also leads to lifetime broadening of the peaks at higher masses. After 36 s, $F^-(H_2O)_k$, $k = 4-6$, are remaining.

$$(H_2O)_n^- + SF_6 \rightarrow F^-(H_2O)_{n-m} + SF_5^• + mH_2O \quad (3)$$

In addition to the cluster species, an intense SF_6^- peak is observed already at 0 s reaction delay. This peak does not change its absolute intensity during the reaction. Moreover, if SF_6^- is ejected from the ICR cell by resonant excitation at its

DOI: 10.1021/acs.jpca.5b06975
J. Phys. Chem. A 2015, 119, 9978−9985

cyclotron frequency, it is not formed again. This shows unambiguously that SF_6^- does not form in collisions with $(H_2O)_n^-$. It can only be formed by attachment of low-energy electrons, which are present in the ICR cell during the fill cycle. The kinetic energy of these electrons must be <0.2 eV, the threshold for formation of SF_5^-,[44] which is not observed in our mass spectra. We cannot rule out that these low-energy electrons come directly from the laser vaporization source; however, we consider it not very probable. First of all, the electrostatic ion transfer together with the time-of-flight parameter for trapping the cluster ions is optimized for masses above 1000 amu, 5 to 6 orders of magnitude higher than the electron mass. Even if electrons make it into the ICR cell, we do not see a realistic mechanism for confining their kinetic energy to <0.2 eV. We therefore think that the source of these low-energy electrons are type II or type III hydrated electrons $(H_2O)_n^-$, that is, negatively charged water clusters that feature very low vertical detachment energies.[87] These species may survive long enough to be trapped inside the ICR cell but lose their electrons quickly afterward. The electrons detach most likely with a kinetic energy determined by the internal temperature of the clusters, which is around 100−150 K.[84] This would place the kinetic energy of the free electrons trapped in the ICR cell in the range of 0.02 eV, far below the threshold for SF_5^- formation and in agreement with the experimental observation.

At a temperature of T = 170 K (Figure 2), the BIRD rate has slowed down by an order of magnitude; therefore, clusters with n = 50−110 are still present after an 8 s reaction delay, Figure 2c.

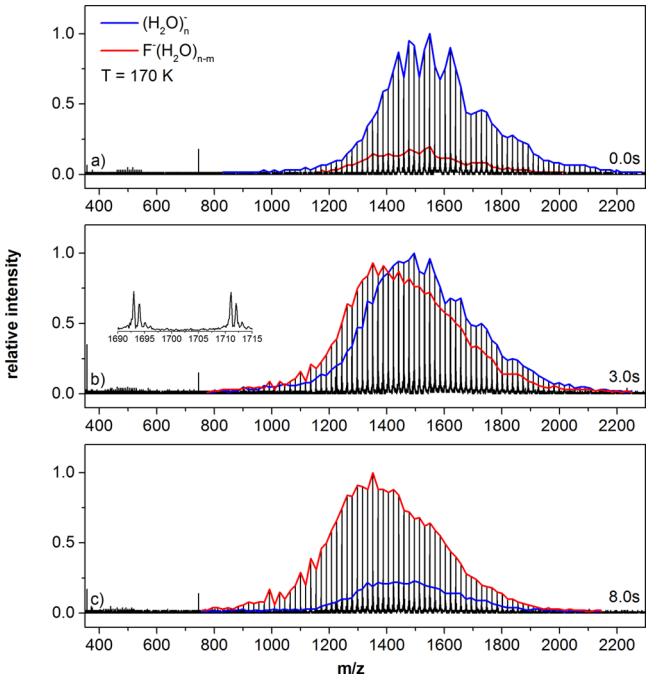

Figure 2. Mass spectra of the reaction of SF_6 with hydrated electrons at 170 K after (a) 0.0, (b) 3.0, and (c) 8.0 s. Again $SF_6^{\bullet-}$ is removed from the cell by resonant excitation. Products are present already at nominal 0.0 s due to the 2 s filling cycle. The intensity fluctuations of the hydrated electron in the 0.0 s mass spectrum are more pronounced than at room temperature. After 3.0 s the reaction is halfway completed. After 8.0 s the reaction is almost finished, and the clusters are still large.

The inset in Figure 2b illustrates the reduced lifetime broadening of the peaks, which improves the overall quality of the data analysis. Also, the intensity fluctuations due to the increased stability of certain cluster sizes are a bit more pronounced, in particular, in the mass spectra of hydrated electrons in Figure 2a. The reaction product is the same as at room temperature, but the rate has almost doubled. This is reasonable because the same reactant pressure is used, which at roughly half the temperature results in a doubling of the number density of the reactant.

To analyze the kinetics and thermochemistry, we plotted the total intensities and average cluster size as a function of time for T = 298 and 170 K in Figures 3 and 4, respectively.

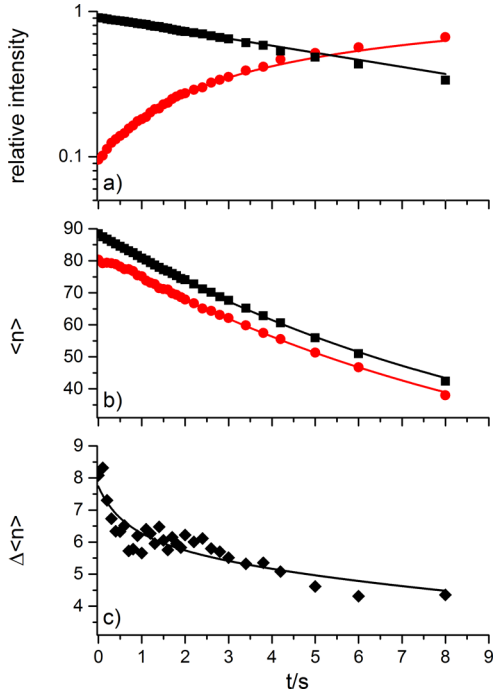

Figure 3. (a) Kinetic and (b,c) nanocalorimetric analysis of the reaction of SF_6 with hydrated electrons at room temperature. Panel a shows the pseudo-first-order fit of the reaction of (filled square) $(H_2O)_n^-$ to (filled circle) $F^-(H_2O)_{n-m}$ with the noise level below 0.001, panel b shows the fit of the cluster sizes for both species, and panel c illustrates the cluster size difference fit (filled diamond).

Kinetics and nanocalorimetry are fitted for the first 8 s of the reaction. The kinetic fits exhibit smooth pseudo-first-order behavior. The nanocalorimetric fit of the average cluster sizes shows that the BIRD rate is reduced by an order of magnitude at 170 K compared with room temperature. Because of the smaller range of cluster sizes displayed in Figure 4b, small fluctuations in the cluster size distribution become more apparent. The fits of the difference of average cluster sizes, Figures 3c and 4c, are also very stable.

To get some insight into a possible cluster-size dependence of the reaction rate, we repeated the experiment at room temperature with a size distribution n = 23−72 (Figure S1 in the Supporting Information). Here the rate is a bit increased, but the number of water molecules evaporating is similar to the large cluster experiments. This data set could be fitted only up to 4 s because blackbody radiation induced electron detachment sets in below n = 30.[76,88]

DOI: 10.1021/acs.jpca.5b06975
J. Phys. Chem. A 2015, 119, 9978−9985

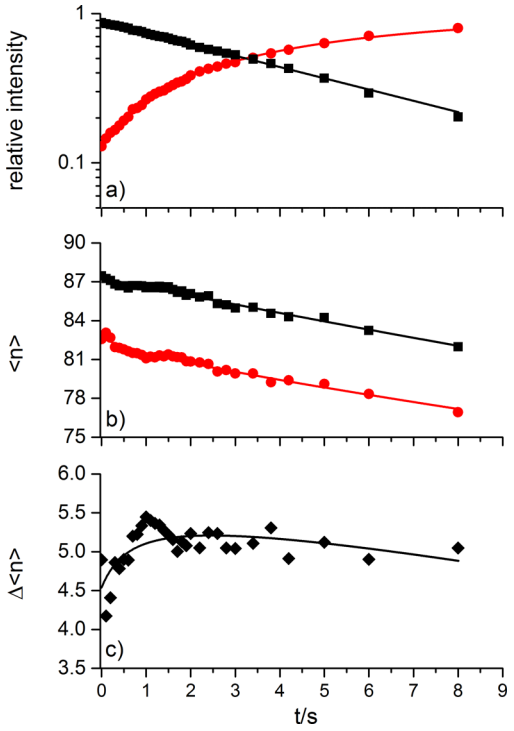

Figure 4. (a) Kinetic and (b,c) nanocalorimetric analysis of the reaction of SF_6 with hydrated electrons at T = 170 K. Panel a shows the pseudo-first-order fit of the reaction (filled square) $(H_2O)_n^-$ to (filled circle) $F^-(H_2O)_{n-m}$ with the noise level below 0.001, panel b shows the fit of the cluster sizes for both species, and panel c illustrates the cluster size difference fit (filled diamond).

The results of all fits are summarized in Table 1. Absolute experimental rate constants are compared with calculated collision rates, namely, the Langevin model of ion-induced dipole capture as part of average dipole orientation theory (ADO)[89] and two approaches that account for the finite size of the clusters, the hard-sphere average dipole orientation (HSA) and the surface charge capture (SCC) model.[90] The experimental rates are so scattered that no clear conclusions can be drawn. Given that in our experience realistic collision rates for hydrated electrons lie between the HSA and SCC model, the efficiency of $F^-(H_2O)_{n-m}$ formation lies around 25%, that is, only one in four collisions is reactive.

Hydration of the electron changes the ionic product from SF_6^- or SF_5^- to $F^-(H_2O)_{n-m}$. This is not surprising because hydration stabilizes the compact F^- ion more than the diffuse electron, making the $F^-(H_2O)_{n-m}$ formation the most exothermic reaction pathway, consistent with the observations in bulk aqueous solution.[54,55] The $SF_5^\bullet$ radical, however, leaves the cluster, so further hydrolysis is not possible, explaining the absence of SOF_4^- or $F^-(HF)_2$ observed in the reaction of SF_6^- with individual water molecules.[53] The SF_6 molecule has a very low solubility in water. Therefore, it interacts via the fluorine atoms with the hydrogen atoms of the water cluster and most likely stays at the cluster surface during the electron transfer. The relatively low reaction efficiency of only 25% suggests that the SF_6 molecule has to hit the cluster in the right area, with the site of the localized hydrated electron pointing toward the collision partner.[91] This is consistent with a surface dipole-bound electron[87,92] and the hydrophobic character of the neutral reactant without a permanent dipole moment. SF_6 attaches the electron only if it collides directly or at least in the vicinity of the electron cloud; otherwise, there are only nonreactive collisions with the cluster. Alternatively, electron transfer is associated with an activation barrier, and re-evaporation of the reactant competes with the reaction.

Nanocalorimetry fits of each reaction yield the number of evaporated water molecules evaporating due to the reaction enthalpy. The fitted values range from 5.0 to 5.7 evaporating water molecules, with a mean value of ΔN_{vap} = 5.4 ± 0.4 water molecules, with a 95% (2σ) confidence interval. An alternative to taking the average value of all fit results is to fit all data sets simultaneously with the same fit parameter ΔN_{vap}. This yields ΔN_{vap} = 5.5, however, without a systematic error bar. The two results differ by only 0.1 water molecules, which is not significant. To be able to work with a statistical error, we use the average value ΔN_{vap} = 5.4 ± 0.4 for our further analysis.

Thermal effects can be neglected because in reaction 3 the heat capacity of ionic and neutral species on the left and right-hand sides of the equation is quite comparable. No temperature dependence is evident from the results. We therefore approximate

$$\Delta H_{298K} = \Delta N_{vap} \Delta E_{vap} = 234 \pm 24 \text{ kJ mol}^{-1} \quad (4)$$

To test the plausibility of these results, we use this value in a thermochemical cycle together with bulk solution phase thermochemistry to calculate the bond dissociation energy of $SF_6(g)$ into $SF_5(g)$ + F(g). To avoid the influence of the high uncertainty of the absolute proton hydration enthalpy,[93] we use the value given by Ishigure and coworkers for the hydration enthalpy of the electron,[94] referenced to the proton. This is combined with the very precisely known dissociation enthalpy of HF(g),[95] the ionization energy of H,[95] and the solution enthalpy of gaseous HF (Table 2).[96]

Table 1. Results of the Kinetic and Nanocalorimetric Analysis of All Data Sets Measured at Temperatures from 150−300 K[a]

T/K	size n	p_{mes}/mbar	k_{abs}/cm^3 s^{-1}	k_{HSA}/cm^3 s^{-1}	k_{SCC}/cm^3 s^{-1}	k_{ADO}/cm^3 s^{-1}	Φ/%	ΔN_{vap}
151	60−126	9.9×10^{-9}	3.0×10^{-10}	6.6×10^{-10}	1.5×10^{-9}	5.0×10^{-10}	28	5.4
170	64−133	9.9×10^{-9}	2.7×10^{-10}	6.8×10^{-10}	1.6×10^{-9}	5.0×10^{-10}	24	5.3
170	53−122	9.9×10^{-9}	2.9×10^{-10}	6.8×10^{-10}	1.6×10^{-9}	5.0×10^{-10}	18	5.7
190	53−122	9.9×10^{-9}	2.9×10^{-10}	7.0×10^{-10}	1.6×10^{-9}	5.0×10^{-10}	25	5.0
226	50−119	9.9×10^{-9}	2.7×10^{-10}	7.4×10^{-10}	1.7×10^{-9}	5.0×10^{-10}	22	5.4
298	64−130	9.9×10^{-9}	3.3×10^{-10}	8.2×10^{-10}	1.8×10^{-9}	5.0×10^{-10}	25	5.5
298	23−72	2.3×10^{-8}	3.7×10^{-10}	8.2×10^{-10}	1.8×10^{-9}	5.0×10^{-10}	28	5.5
298	53−123	9.7×10^{-9}	2.6×10^{-10}	8.2×10^{-10}	1.8×10^{-9}	5.0×10^{-10}	20	5.3

[a]Temperature T of radiation shield and reactant gas, the reactant pressure p in mbar, absolute reaction rate coefficient $k_{abs}$and collision rates according to the hard sphere average dipole orientation model k_{HSA}, the surface charge capture model k_{SCC}, and average dipole orientation theory k_{ADO}, the reaction efficiency $\Phi = 2k_{abs}/(k_{HSA} + k_{SCC})$, and the number of evaporated water molecules ΔN_{vap}.

DOI: 10.1021/acs.jpca.5b06975
J. Phys. Chem. A 2015, 119, 9978−9985

Table 2. Thermochemical Cycle for the F_5S-F Bond Dissociation Energy

reaction	ΔH_{298K}/kJ mol^{-1}	ref
$H^+_{(g)} + e^-_{(g)} \rightarrow H^+_{(aq)} + e^-_{(aq)}$	−1261.9 ± 3.8	94
$H^+_{(aq)} + F^-_{(aq)} \rightarrow HF_{(g)}$	+61.5 ± 0.8	.
$HF_{(g)} \rightarrow H^\bullet_{(g)} + F^\bullet_{(g)}$	+570.7 ± 0.8	95
$H^\bullet_{(g)} \rightarrow H^+_{(g)} + e^-_{(g)}$	+1318.4 ± 0.0	95
$SF_{6(g)} + e^-_{(aq)} \rightarrow SF_5^\bullet{}_{(g)} + F^-_{(aq)}$	−234 ± 24	this work
$SF_{6(g)} \rightarrow SF_5^\bullet{}_{(g)} + F_{(g)}$	+455 ± 24	sum of all above

High-level ab initio calculations by Bauschlicher and Ricca yield a value of 453 kJ mol^{-1},[34] and all high-level calculations in the literature lie within 10 kJ mol^{-1}.[32] The critical evaluation of experimental data by Tsang and Herron for the 298 K bond dissociation enthalpy yields 420 ± 10 kJ mol^{-1}.[40] Experimental values are consistently lower in the literature than theory, as previously discussed.[33,36] Our value is thus the first experimental determination of the F_5S−F bond dissociation enthalpy that is in agreement with the calculations and consequently is higher than the experimental estimate by Tsang and Herron.

From this, we can derive a value for the electron affinity of $SF5^\bullet_{(g)}$. Troe, Miller, and Viggiano reported an accurate modeling of the dissociative electron attachment to SF_6 in the gas phase to yield SF_5^- and F, $E_{0,dis}$ = −39.6 ± 4.8 kJ mol^{-1} (Table 3).[22] This yields EA(SF_5) = 4.27 ± 0.25 eV.

Table 3. Thermochemical Cycle for the Electron Affinity of $SF_5\bullet$

reaction	ΔE_0/kJ mol^{-1}	ref
$SF_{6(g)} \rightarrow SF_5^\bullet{}_{(g)} + F^\bullet_{(g)}$	+452 ± 24	this work, converted to 0 K with ref 34
$SF_5^-{}_{(g)} + F^\bullet_{(g)} \rightarrow SF_{6(g)} + e^-_{(g)}$	−39.6 ± 4.8	22
$SF_5^-{}_{(g)} \rightarrow SF_5^\bullet{}_{(g)} + e^-_{(g)}$	+412 ± 24	sum of all above

Again, this value agrees within error limits with G2(MP2) calculations by Cheung et al.[35] and lies above the highest experimental value reported by Chen and Chen.[28] It is tempting to state that nanocalorimetry is superior for the determination of adiabatic reaction enthalpies because the product species relax in the water cluster and dissipate their excess energy before evaporation if the ergodicity assumption is fulfilled;[64] however, the method is not yet highly accurate: We do not know the influence of a possible size dependence of the reaction rate on the result, and also temperature effects are not fully understood. With this caveat in mind, we can state that nanocalorimetry together with literature data for bulk aqueous solution yields meaningful thermochemical values.

4. CONCLUSIONS

Unlike electron attachment reactions of the SF_6 molecule without solvent shell, the reaction of gas-phase hydrated electrons with SF_6 leads to the formation of hydrated fluoride $F^-(H_2O)_{n-m}$ and an $SF_5^\bullet$ radical, which evaporates from the cluster. The most intense peak in the mass spectra is the bare SF_6^- anion, which indicates the presence of low-energy electrons in the ICR cell. These electrons are formed from type II or type III hydrated electrons that quickly detach the electron. The reaction enthalpy was analyzed with nanocalorimetry. In combination with bulk thermochemistry, the SF_5−F bond dissociation enthalpy was derived as −455 ± 24 kJ mol^{-1}. This is consistent with literature values from theory as well as experiment. This study thus shows that nanocalorimetry in combination with literature thermochemistry for bulk aqueous solution provides realistic thermochemical values. This does not show that bulk behavior is reached with clusters with around 100 water molecules, but it does confirm that the thermochemistry of reactant and product clusters differs quantitatively in the same way from the bulk.

■ ASSOCIATED CONTENT

Supporting Information

The Supporting Information is available free of charge on the ACS Publications website at DOI: 10.1021/acs.jpca.5b06975.

Kinetic and nanocalorimetric analysis of the reaction of SF_6 with hydrated electrons at room temperature and smaller cluster sizes (Figure S1). Temperature dependence of calculated collision rates and experimental reaction rate constant (Figure S2). Details of the determination of k_{abs} and pressure calibration. (PDF)

■ AUTHOR INFORMATION

Corresponding Author

*E-mail: martin.beyer@uibk.ac.at.

Notes

The authors declare no competing financial interest.

■ ACKNOWLEDGMENTS

Financial support by the Deutsche Forschungsgemeinschaft, grant no. BE2505/4-3, is gratefully acknowledged.

■ DEDICATION

Dedicated to the memory of PD Dr. Oliver Hampe, for his contributions to the thermochemistry of ion−molecule reactions.

■ REFERENCES

(1) Champion, R. L.; Dyakov, I. V.; Peko, B. L.; Wang, Y. Collisional Decomposition of the Sulfur Hexaflouride Anion (SF_6^-). *J. Chem. Phys.* **2001**, *115*, 1765−1768.

(2) Christophorou, L. G.; Olthoff, J. K.; Van Brunt, R. J. Sulfur Hexafluoride and the Electric Power Industry. *IEEE Electr. Insul. Mag.* **1997**, *13*, 20−24.

(3) Kline, L. E.; Davies, D. K.; Chen, C. L.; Chantry, P. J. Dielectric Properties for SF_6 and SF_6 Mixtures Predicted from Basic Data. *J. Appl. Phys.* **1979**, *50*, 6789−6796.

(4) Morrow, R. A Survey of the Electron and Ion Transport Properties of SF_6. *IEEE Trans. Plasma Sci.* **1986**, *14*, 234−239.

(5) Odom, R. W.; Smith, D. L.; Futrell, J. H. A Study of Electron Attachment to SF_6 and Auto-Detachment and Stabilization of SF_6^-. *J. Phys. B: At. Mol. Phys.* **1975**, *8*, 1349−1366.

(6) Morris, R. A.; Miller, T. M.; Viggiano, A. A.; Paulson, J. F.; Solomon, S.; Reid, G. Effects of Electron and Ion Reactions on Atmospheric Lifetimes of Fully Fluorinated Compounds. *J. Geophys. Res.* **1995**, *100*, 1287−1294.

(7) Maiss, M.; Brenninkmeijer; Carl, A. M. Atmospheric SF_6: Trends, Sources, and Prospects. *Environ. Sci. Technol.* **1998**, *32*, 3077−3086.

(8) Huey, L. G.; Hanson, D. R.; Howard, C. J. Reactions of SF_6^- and I^- with Atmospheric Trace Gases. *J. Phys. Chem.* **1995**, *99*, 5001−5008.

(9) Maiss, M.; Levin, I. Global Increase of SF_6 observed in the Atmosphere. *Geophys. Res. Lett.* **1994**, *21*, 569−572.

(10) Margreiter, D.; Deutsch, H.; Schmidt, M.; Märk, T. D. Electron Impact Ionization Cross Sections of Molecules. *Int. J. Mass Spectrom. Ion Processes* **1990**, *100*, 157−176.

DOI: 10.1021/acs.jpca.5b06975
J. Phys. Chem. A 2015, 119, 9978−9985

(11) Margreiter, D.; Walder, G.; Deutsch, H.; Poll, H. U.; Winkler, C.; Stephan, K.; Märk, T. D. Electron Impact Ionization Cross Sections of Molecules. *Int. J. Mass Spectrom. Ion Processes* **1990**, *100*, 143−156.
(12) Howard, C. J.; Fehsenfeld, F. C.; McFarland, M. Negative Ion−Molecule Reactions with Atomic Hydrogen in the Gas Phase at 296 K. *J. Chem. Phys.* **1974**, *60*, 5086−5089.
(13) Arnold, S. T.; Seeley, J. V.; Williamson, J. S.; Mundis, P. L.; Viggiano, A. A. New Apparatus for the Study of Ion−Molecule Reactions at Very High Pressure (25−700 Torr): A Turbulent Ion Flow Tube (TIFT) Study of the Reaction of SF_6^-+SO_2. *J. Phys. Chem. A* **2000**, *104*, 5511−5516.
(14) Arnold, S. T.; Viggiano, A. A. Turbulent Ion Flow Tube Study of the Cluster-Mediated Reactions of SF_6^- with H_2O, CH_3OH, and C_2H_5OH from 50 to 500 Torr. *J. Phys. Chem. A* **2001**, *105*, 3527−3531.
(15) Bopp, J. C.; Roscioli, J. R.; Johnson, M. A.; Miller, T. M.; Viggiano, A. A.; Villano, S. M.; Wren, S. W.; Lineberger, W. C. Spectroscopic Characterization of the Isolated SF_6^- and $C_4F_8^-$ Anions: Observation of Very Long Harmonic Progressions in Symmetric Deformation Modes upon Photodetachment. *J. Phys. Chem. A* **2007**, *111*, 1214−1221.
(16) Märk, T. D. Free Electron Attachment to Van Der Waals Clusters. *Int. J. Mass Spectrom. Ion Processes* **1991**, *107*, 143−163.
(17) Fehsenfeld, F. C. Electron Attachment to SF_6. *J. Chem. Phys.* **1970**, *53*, 2000−2004.
(18) van Brunt, R. J.; Herron, J. T. Plasma Chemical Model for Decomposition of SF_6 in a Negative Glow Corona Discharge. *Phys. Scr.* **1994**, *T53*, 9−29.
(19) Christophorou, L. G.; Olthoff, J. K. Electron Attachment Cross Sections and Negative Ion States of SF_6. *Int. J. Mass Spectrom.* **2001**, *205*, 27−41.
(20) Steill, J. D.; Oomens, J.; Eyler, J. R.; Compton, R. N. Gas-Phase Infrared Multiple Photon Dissociation Spectroscopy of Isolated SF_6^- and SF_5^- Anions. *J. Chem. Phys.* **2008**, *129*, 244302(3−8).
(21) Fenzlaff, M.; Gerhard, R.; Illenberger, E. Associative and Dissociative Electron Attachment by SF_6 and SF_5Cl. *J. Chem. Phys.* **1988**, *88*, 149−155.
(22) Troe, J.; Miller, T. M.; Viggiano, A. A. Low-energy Electron Attachment to SF_6. II. Temperature and Pressure Dependences of Dissociative Attachment. *J. Chem. Phys.* **2007**, *127*, 244304(1−13).
(23) Troe, J.; Miller, T. M.; Viggiano, A. A. Communication: Revised Electron Affinity of SF_6 from Kinetic Data. *J. Chem. Phys.* **2012**, *136*, 121102(1−3).
(24) Lifshitz, C.; Tiernan, T. O.; Hughes, B. M. Electron Affinities from Endothermic Negative-Ion Charge-Transfer Reactions. IV. SF_6, Selected Fluorocarbons and Other Polyatomic Molecules. *J. Chem. Phys.* **1973**, *59*, 3182−3192.
(25) Chen, Edward C. M.; Shuie, L.-R.; Desai D'sa, E.; Batten, C. F.; Wentworth, W. E. The Negative Ion States of Sulfur Hexafluoride. *J. Chem. Phys.* **1988**, *88*, 4711−4719.
(26) Gutsev, G. L.; Bartlett, R. J. Adiabatic Electron Affinities of PF_5 and SF_6: a Coupled-Cluster Study 5 6. *Mol. Phys.* **1998**, *94*, 121−125.
(27) Miller, T. M.; Viggiano, A. A.; Troe, J. Electron Attachment to SF_6 under well Defined Conditions: Comparison of Statistical Modeling Results to Experiments. *J. Phys. Conf. Ser.* **2008**, *115*, 012019.
(28) Chen, E. C. M.; Chen, E. S. Electron Affinities and Activation Energies for Reactions with Thermal Electrons: SF_6 and SF_5. *Phys. Rev. A: At., Mol., Opt. Phys.* **2007**, *76*, 032508(1−12).
(29) Eisfeld, W. Highly Accurate Determination of the Electron Affinity of SF_6 and Analysis of Structure and Photodetachment Spectrum of SF_6^-. *J. Chem. Phys.* **2011**, *134*, 054303(1−13).
(30) Eisfeld, W. Erratum: "Highly Accurate Determination of the Electron Affinity of SF_6 and Analysis of Structure and Photodetachment Spectrum of SF_6. *J. Chem. Phys.* **2011**, *134*, 129903.
(31) Karton, A.; Martin, J. M. L. Comment on "Revised Electron Affinity of SF_6 from Kinetic Data. *J. Chem. Phys.* **2012**, *136*, 197101.
(32) Gutsev, G. L. The Structure of the SF_6 Molecule and the SF_6^- Anion Excited States. *B. Russ. Acad. Sci. Chem.* **1992**, *41*, 504−510.
(33) Woon, D. E.; Dunning, T. H. Theory of Hypervalency: Recoupled Pair Bonding in $SF_{(n)}$ (n = 1−6). *J. Phys. Chem. A* **2009**, *113*, 7915−7926.
(34) Bauschlicher, C. W.; Ricca, A. Accurate Heats of Formation for SF_n, SF_n^+, and SF_n^- for n = 1−6. *J. Phys. Chem. A* **1998**, *102*, 4722−4727.
(35) Cheung, Y.-S.; Chen, Y.-J.; Ng, C. Y.; Chiu, S.-W.; Li, W.-K. Combining Theory with Experiment: Assessment of the Thermochemistry of SF_n, SF_n^+, and SF_n^-, n = 1−6. *J. Am. Chem. Soc.* **1995**, *117*, 9725−9733.
(36) Irikura, K. K. Structure and Thermochemistry of Sulfur Fluorides SF_n (n = 1−5) and their Ions SF_n^+ (n = 1−5). *J. Chem. Phys.* **1995**, *102*, 5357−5367.
(37) Grant, D. J.; Matus, M. H.; Switzer, J. R.; Dixon, D. A.; Francisco, J. S.; Christe, K. O. Bond Dissociation Energies in Second-Row Compounds. *J. Phys. Chem. A* **2008**, *112*, 3145−3156.
(38) Miller, T. M.; Arnold, S. T.; Viggiano, A. A. G3 and G2 Thermochemistry of Sulfur Fluoride Neutrals and Anions. *Int. J. Mass Spectrom.* **2003**, *227*, 413−420.
(39) Kiang, T.; Zare, R. N. Stepwise Bond Dissociation Energies in Sulfur Hexafluoride. *J. Am. Chem. Soc.* **1980**, *102*, 4024−4029.
(40) Tsang, W.; Herron, J. T. Kinetics and Thermodynamics of the Reaction $SF_6 \rightleftarrows SF_5$+F. *J. Chem. Phys.* **1992**, *96*, 4272−4280.
(41) Braun, M.; Barsotti, S.; Marienfeld, S.; Leber, E.; Weber, J. M.; Ruf, M.-W.; Hotop, H. High Resolution Study of Anion Formation in Low-Energy Electron Attachment to SF_6 Molecules in a Seeded Supersonic Beam. *Eur. Phys. J. D* **2005**, *35*, 177−191.
(42) Dillard, J. G.; Rhyne, T. C. Reactions of Gaseous Inorganic Negative Ions. II. SF_6^- and Nonmetal Fluorides. *Inorg. Chem.* **1971**, *10*, 730−735.
(43) Graupner, K.; Field, T. A.; Mauracher, A.; Scheier, P.; Bacher, A.; Denifl, S.; Zappa, F.; Märk, T. D. Fragmentation of Metastable $SF_6^{(-*)}$ Ions with Microsecond Lifetimes in Competition with Autodetachment. *J. Chem. Phys.* **2008**, *128*, 104304.
(44) Chen, C. L.; Chantry, P. J. Photon-Enhanced Dissociative Electron Attachment in SF_6 and its Isotopic Selectivity. *J. Chem. Phys.* **1979**, *71*, 3897−3907.
(45) Sauers, I.; Harman, G. A Mass Spectrometric Study of Positive and Negative Ion Formation in an SF_6 Corona. II. Influence of Water and SF_6 Neutral by-Products. *J. Phys. D: Appl. Phys.* **1992**, *25*, 774−782.
(46) Streit, G. E. Negative Ion Chemistry and the Electron Affinity of SF_6. *J. Chem. Phys.* **1982**, *77*, 826−833.
(47) Christophorou, L. G.; Olthoff, J. K. Electron Attachment Cross Sections and Negative Ion States of SF_6. *Int. J. Mass Spectrom.* **2001**, *205*, 27−41.
(48) Weik, F.; Illenberger, E. Dissociative Electron Attachment and Charging of SF_6 Adsorbed on Rare-Gas Films. *J. Chem. Phys.* **1998**, *109*, 6079−6085.
(49) Wang, Y.; Champion, R. L.; Doverspike, L. D.; Olthoff, J. K.; Van Brunt, R. J. Collisional Electron Detachment and Decomposition Cross Sections for SF_6^-, SF_5^-, and F^- on SF_6 and Rare Gas Targets. *J. Chem. Phys.* **1989**, *91*, 2254−2260.
(50) Van Brunt, R. J.; Herron, J. T. Fundamental Processes of SF_6 Decomposition and Oxidation in Glow and Corona Discharges. *IEEE Trans. Electr. Insul.* **1990**, *25*, 75−94.
(51) Sieck, L. W.; Van Brunt, Richard J. Rate Constants for Fluoride Transfer from Sulfur Hexafluoride (1-) to Fluorinated Gases and Sulfur Dioxide: Temperature Dependence and Implications for Electrical Discharges in Sulfur Hexafluoride. *J. Phys. Chem.* **1988**, *92*, 708−713.
(52) Lobring, K. C.; Check, C. E.; Gilbert, T. M.; Sunderlin, L. S. New Measurements of the Thermochemistry of SF_5^- and SF_6^-. *Int. J. Mass Spectrom.* **2003**, *227*, 361−372.
(53) Arnold, S. T.; Viggiano, A. A. Turbulent Ion Flow Tube Study of the Cluster-Mediated Reactions of SF_6^- with H_2O, CH_3OH, and

DOI: 10.1021/acs.jpca.5b06975
J. Phys. Chem. A 2015, 119, 9978−9985

C_2H_5OH from 50 to 500 Torr. *J. Phys. Chem. A* **2001**, *105*, 3527−3531.
(54) Asmus, K. D.; Fendler, J. H. Reaction of Sulfur Hexafluoride with Hydrated Electrons. *J. Phys. Chem.* **1968**, *72*, 4285−4289.
(55) Haygarth, K.; Bartels, D. M. Neutron and Beta/Gamma Radiolysis of Water up to Supercritical Conditions. 2. SF_6 as a Scavenger for Hydrated Electron. *J. Phys. Chem. A* **2010**, *114*, 7479−7484.
(56) Arshadi, M.; Yamdagni, R.; Kebarle, P. Hydration of the Halide Negative Ions in the Gas Phase. II. Comparison of Hydration Energies for the Alkali Positive and Halide Negative Ions. *J. Phys. Chem.* **1970**, *74*, 1475−1482.
(57) Castleman, A. W.; Keesee, R. G. Clusters: Bridging the Gas and Condensed Phases. *Acc. Chem. Res.* **1986**, *19*, 413−419.
(58) Lee, N.; Keesee, R.; Castleman, A. On the Correlation of Total and Partial Enthalpies of Ion Solvation and the Relationship to the Energy Barrier to Nucleation. *J. Colloid Interface Sci.* **1980**, *75*, 555−565.
(59) Donald, W. A.; Leib, R. D.; O'Brien, J. T.; Bush, M. F.; Williams, E. R. Absolute Standard Hydrogen Electrode Potential Measured by Reduction of Aqueous Nanodrops in the Gas Phase. *J. Am. Chem. Soc.* **2008**, *130*, 3371−3381.
(60) Donald, W. A.; Leib, R. D.; O'Brien, J. T.; Holm, A. I. S.; Williams, E. R. Nanocalorimetry in Mass Spectrometry: A Route to Understanding Ion and Electron Solvation. *Proc. Natl. Acad. Sci. U. S. A.* **2008**, *105*, 18102−18107.
(61) Donald, W. A.; Leib, R. D.; O'Brien, J. T.; Williams, E. R. Directly Relating Gas-Phase Cluster Measurements to Solution-Phase Hydrolysis, the Absolute Standard Hydrogen Electrode Potential, and the Absolute Proton Solvation Energy. *Chem. - Eur. J.* **2009**, *15*, 5926−5934.
(62) Donald, W. A.; Leib, R. D.; Demireva, M.; O'Brien, J. T.; Prell, J. S.; Williams, E. R. Directly Relating Reduction Energies of Gaseous $Eu(H_2O)_n^{3+}$, n = 55−140, to Aqueous Solution: The Absolute SHE Potential and Real Proton Solvation Energy. *J. Am. Chem. Soc.* **2009**, *131*, 13328−13337.
(63) Leib, R. D.; Donald, W. A.; Bush, M. F.; O'Brie, J. T.; Williams, E. R. Internal Energy Deposition in Electron Capture Dissociation Measured Using Hydrated Divalent Metal Ions as Nanocalorimeters. *J. Am. Chem. Soc.* **2007**, *16*, 4894−4895.
(64) Höckendorf, R. F.; Balaj, O. P.; van der Linde, Christian; Beyer, M. K. Thermochemistry from Ion−Molecule Reactions of Hydrated Ions in the Gas Phase: a New Variant of Nanocalorimetry Reveals Product Energy Partitioning. *Phys. Chem. Chem. Phys.* **2010**, *12*, 3772−3779.
(65) Höckendorf, R. F.; Balaj, O. P.; Beyer, M. K. Competition between Birch Reduction and Fluorine Abstraction in Reactions of Hydrated Electrons $(H_2O)_n^-$ with the Isomers of Di- and Trifluorobenzene. *Phys. Chem. Chem. Phys.* **2011**, *13*, 8924−8930.
(66) Akhgarnusch, A.; Beyer, M. K. Electron Transfer Reactions of Nitromethane, Acetaldehyde and Benzaldehyde with $(H_2O)_n^-$, $CO_2^{\cdot-}(H_2O)_n$, and $O_2^-(H_2O)_n$, $n < 110$, in the Gas Phase. *Int. J. Mass Spectrom.* **2014**, *365*−*366*, 295−300.
(67) Akhgarnusch, A.; Höckendorf, R. F.; Hao, Q.; Jäger, K. P.; Siu, C.-K.; Beyer, M. K. Carboxylation of Methyl Acrylate by Carbon Dioxide Radical Anions in Gas-Phase Water Clusters. *Angew. Chem., Int. Ed.* **2013**, *52*, 9327−9330.
(68) Balaj, O. P.; Berg, C. B.; Reitmeier, S. J.; Bondybey, V. E.; Beyer, M. K. A Novel Design of a Temperature-Controlled FT-ICR Cell for Low-Temperature Black-Body Infrared Radiative Dissociation (BIRD) Studies of Hydrated Ions. *Int. J. Mass Spectrom.* **2009**, *279*, 5−9.
(69) Allemann, M.; Kellerhals, H.; Wanczek, K. P. High Magnetic Field Fourier Transform Ion Cyclotron Resonance Spectroscopy. *Int. J. Mass Spectrom. Ion Phys.* **1983**, *46*, 139−142.
(70) Kofel, P.; Allemann, M.; Kellerhals, H.; Wanczek, K.-P. Time-of-Flight ICR Spectrometry. *Int. J. Mass Spectrom. Ion Processes* **1986**, *72*, 53−61.
(71) Berg, C.; Schindler, T.; Niedner-Schatteburg, G.; Bondybey, V. E. Reactions of Simple Hydrocarbons with Nb^+_n: Chemisorption and Physisorption on Ionized Niobium Clusters. *J. Chem. Phys.* **1995**, *102*, 4870−4884.
(72) Bondybey, V. E.; English, J. H. Laser Induced Fluorescence of Metal Clusters Produced by Laser Vaporization: Gas Phase Spectrum of Pb_2. *J. Chem. Phys.* **1981**, *74*, 6978−6979.
(73) Dietz, T. G.; Duncan, M. A.; Powers, D. E.; Smalley, R. E. Laser Production of Supersonic Metal Cluster Beams. *J. Chem. Phys.* **1981**, *74*, 6511−6512.
(74) Maruyama, S.; Anderson, L. R.; Smalley, R. E. Direct Injection Supersonic Cluster Beam Source for FT-ICR Studies of Clusters. *Rev. Sci. Instrum.* **1990**, *61*, 3686−3693.
(75) Beyer, M.; Berg, C.; Görlitzer, H. W.; Schindler, T.; Achatz, U.; Albert, G.; Niedner-Schatteburg, G.; Bondybey, V. E. Fragmentation and Intracluster Reactions of Hydrated Aluminum Cations $Al^+(H_2O)_n$, n = 3−50. *J. Am. Chem. Soc.* **1996**, *118*, 7386−7389.
(76) Beyer, M. K.; Fox, B. S.; Reinhard, B. M.; Bondybey, V. E. Wet Electrons and How to Dry Them. *J. Chem. Phys.* **2001**, *115*, 9288−9297.
(77) Schindler, T.; Berg, C.; Niedner-Schatteburg, G.; Bondybey, V. E. Gas-Phase Reactivity of Sulfur Cluster Cations and Anions by FT-ICR Investigations. *Ber. Bunsen-Ges. Phys. Chem.* **1992**, *96*, 1114−1120.
(78) Fox, B. S.; Beyer, M. K.; Bondybey, V. E. Black Body Fragmentation of Cationic Ammonia Clusters. *J. Phys. Chem. A* **2001**, *105*, 6386−6392.
(79) Hampe, O.; Karpuschkin, T.; Vonderach, M.; Weis, P.; Yu, Y. M.; Gan, L. B.; Klopper, W.; Kappes, M. M. Heating a Bowl of Single-Molecule-Soup: Structure and Desorption Energetics of Water-Encapsulated Open-Cage [60] Fullerenoid Anions in the Gas-Phase. *Phys. Chem. Chem. Phys.* **2011**, *13*, 9818−9823.
(80) Lee, S. W.; Freivogel, P.; Schindler, T.; Beauchamp, J. L. Freeze-Dried Biomolecules: FT-ICR Studies of the Specific Solvation of Functional Groups and Clathrate Formation Observed by the Slow Evaporation of Water from Hydrated Peptides and Model Compounds in the Gas Phase. *J. Am. Chem. Soc.* **1998**, *120*, 11758−11765.
(81) Schindler, T.; Berg, C.; Niedner-Schatteburg, G.; Bondybey, V. E. Protonated Water Clusters and their Black Body Radiation Induced Fragmentation. *Chem. Phys. Lett.* **1996**, *250*, 301−308.
(82) Schnier, P. D.; Price, W. D.; Jockusch, R. A.; Williams, E. R. Blackbody Infrared Radiative Dissociation of Bradykinin and its Analogues: Energetics, Dynamics, and Evidence for Salt-Bridge Structures in the Gas Phase. *J. Am. Chem. Soc.* **1996**, *118*, 7178−7189.
(83) Sena, M.; Riveros, J. M.; Nibbering, N. M. M. The Unimolecular Dissociation of the Molecular Ion of Acetophenone Induced by Thermal-Radiation. *Rapid Commun. Mass Spectrom.* **1994**, *8*, 1031−1034.
(84) Dunbar, R. C. BIRD (Blackbody Infrared Radiative Dissociation): Evolution, Principles, and Applications. *Mass Spectrom. Rev.* **2004**, *23*, 127−158.
(85) Hock, C.; Schmidt, M.; Kuhnen, R.; Bartels, C.; Ma, L.; Haberland, H.; v.Issendorff, B. Calorimetric Observation of the Melting of Free Water Nanoparticles at Cryogenic Temperatures. *Phys. Rev. Lett.* **2009**, *103*, 073401.
(86) Donald, W. A.; Leib, R. D.; Demireva, M.; Negru, B.; Neumark, D. M.; Williams, E. R. Average Sequential Water Molecule Binding Enthalpies of $M(H_2O)_{(19-124)}^{2+}$ (M = Co, Fe, Mn, and Cu) Measured with Ultraviolet Photodissociation at 193 and 248 nm. *J. Phys. Chem. A* **2011**, *115*, 2−12.
(87) Young, R. M.; Neumark, D. M. Dynamics of Solvated Electrons in Clusters. *Chem. Rev.* **2012**, *112*, 5553−5577.
(88) Arnold, S. T.; Morris, R. A.; Viggiano, A. A. Competition between Electron Detachment and Monomer Evaporation in the Thermal Destruction of Hydrated Electron Clusters. *J. Chem. Phys.* **1995**, *103*, 9242−9248.
(89) Su, T.; Bowers, M. T. Parameterization of Average Dipole Orientation Theory - Temperature-Dependence. *Int. J. Mass Spectrom. Ion Phys.* **1975**, *17*, 211−212.
(90) Kummerlöwe, G.; Beyer, M. K. Rate Estimates for Collisions of Ionic Clusters with Neutral Reactant Molecules. *Int. J. Mass Spectrom.* **2005**, *244*, 84−90.

DOI: 10.1021/acs.jpca.5b06975
J. Phys. Chem. A 2015, 119, 9978−9985

(91) Mikosch, J.; Weidemüller, M.; Wester, R. On the Dynamics of Chemical Reactions of Negative. *Int. Rev. Phys. Chem.* **2010**, *29*, 589−617.
(92) Uhlig, F.; Herbert, J. M.; Coons, M. P.; Jungwirth, P. Optical Spectroscopy of the Bulk and Interfacial Hydrated Electron from Ab Initio Calculations. *J. Phys. Chem. A* **2014**, *118*, 7507−7515.
(93) Donald, W. A.; Demireva, M.; Leib, R. D.; Aiken, M. J.; Williams, E. R. Electron Hydration and Ion-Electron Pairs in Water Clusters Containing Trivalent Metal Ions. *J. Am. Chem. Soc.* **2010**, *132*, 4633−4640.
(94) Shiraishi, H.; Sunaryo, G. R.; Ishigure, K. Temperature Dependence of Equilibrium and Rate Constants of Reactions Inducing Conversion between Hydrated Electron and Atomic Hydrogen. *J. Phys. Chem.* **1994**, *98*, 5164−5173.
(95) Linstrom, P. J.; Mallard, W. G. (Hg.) *NIST Chemistry WebBook, NIST Standard Reference Database Number 69*; National Institute of Standards and Technology: Gaithersburg, MD, 2005.
(96) Parker, V. B. *Thermal Properties of Aqueous Uni-Univalent Electrolytes: National Standard Reference Data Series*; National Bureau of Standards 2 (Category 5 - Thermodynamic and Transport Properties): Washington, DC, 1965.

DOI: 10.1021/acs.jpca.5b06975
J. Phys. Chem. A 2015, 119, 9978−9985